ELSEVIER

Catalysis Today 39 (1998) 351–361

CATALYSIS TODAY

On-line characterization by EXAFS of tin promoted platinum graphite catalysts in the aqueous phase

H.H.C.M. Pinxt[a], B.F.M. Kuster[a,*], D.C. Koningsberger[b], G.B. Marin[a]

[a]*Eindhoven University of Technology, Schuit Institute of Catalysis, Laboratorium voor Chemische Technologie, PO Box 513, 5600 MB Eindhoven, Netherlands*

[b]*Utrecht University, Debye Institute, Laboratory of Inorganic Chemistry, PO Box 80083, 3508 TB Utrecht, Netherlands*

Abstract

The structure of tin promoted graphite supported platinum catalysts has been studied with extended X-ray absorption fine structure spectroscopy (EXAFS). A newly developed EXAFS cell allows on-line characterization avoiding contact to ambient or drying. Hereto catalyst samples are transferred from a slurry reactor to the EXAFS cell forming a "bed" of catalyst particles in the EXAFS cell. The cell design was based on considerations concerning possible mass transport limitations while performing reactions in the liquid phase. The structures of the tin promoted platinum catalysts were investigated directly after preparation, drying, treatments with hydrogen (363 K) and oxygen (RT) in aqueous phase and a hydrogen gas treatment at 573 K at both the Pt L_{III} and the Sn K-edge. After preparation, under aqueous hydrogen, reduced platinum can be detected with three coordinations: Pt–Pt, Pt–C and Pt–Sn. Tin appears to be partly oxidic showing a Sn–O and a Sn–Pt coordination. A treatment with aqueous oxygen or exposure to ambient leads to oxidized platinum and tin. At the Pt L_{III}-edge only a Pt–Pt and Pt–O coordination for platinum are detected. At the Sn K-edge tin has only a Sn–O coordination. An aqueous treatment with hydrogen at 363 K reduces platinum showing, however, different coordination numbers for the Pt–Pt and Pt–Sn coordination. Tin only shows a Sn–O coordination. A treatment with hydrogen at 573 K reduces both the platinum and the tin. Platinum shows a Pt–Pt, Pt–C and Pt–Sn coordination. Tin shows a Sn–Pt and Sn–O coordination indicating tin deposition on the platinum, tin being bonded via oxygen to the graphite support. Reductive treatments in the aqueous phase appear to reduce platinum and only the tin deposited on the platinum. The effects of drying and consecutive reductive treatments could only be studied since the developed EXAFS cell allowed catalyst preparation and treatments avoiding contact to ambient. © 1998 Elsevier Science B.V.

Keywords: Platinum; Tin; EXAFS; Aqueous; Oxygen transport; Oxidation; Reduction

1. Introduction

Noble metal catalyzed oxidations in the aqueous phase using dioxygen can be applied to the conversion of carbohydrates as a renewable resource. In fine-chemistry noble metal catalysis replaces polluting stoichiometric oxidation agents and in waste water purification it enables lower operating temperatures for wet oxidation. The addition of promoter metals has a large influence on activity, selectivity and stability of the catalyst [1]. In order to understand the phenomena involved, in situ characterization of the catalyst is highly desirable. Extended X-ray absorption fine

*Corresponding author. Tel.: +31 40 2472850; fax: +31 40 2446653; e-mail: margriet@chem.tue.nl.

PII S0920-5861(97)00127-2

structure spectroscopy (EXAFS) is a method which can be applied to liquid systems. EXAFS will give information about the structure of the active catalytic surface on condition of a high dispersion, i.e. when most of the metal atoms are surface atoms. Van den Tillaart [2,3] reported on the use of EXAFS to characterize a platinum catalyst in water, describing the effect of aqueous oxidative and reductive treatments at different pH on the catalyst structure. A conventional EXAFS-cell, where the catalyst sample is present as a pressed wafer, was used. Working with a pressed wafer gives reliable EXAFS-results, however, in liquid systems, it has the disadvantage of long (pre)-treatment times necessary due to diffusional limitations. In more recent studies on promoted platinum catalysts it was found that the (pre)treatment conditions had a large influence on the reaction kinetics observed. Especially drying and exposure to ambient air, necessary to make pressed wafers, resulted in changes of the activity and the selectivity. Furthermore, using electrochemical techniques, it appeared that during reaction the promoter metal can change location within the catalyst, being deposited on the support or on the surface of the active metal [4].

These phenomena, together with the long treatment times, when using pressed wafers, lead to the development of a new EXAFS cell for on-line characterization where a catalyst with a typical powder diameter of 20 μm can be treated in the slurry phase and transferred to the EXAFS cell where it settles as a packed catalyst bed of sufficient uniformity.

Before results on the application of EXAFS for the characterization of a graphite supported Pt/Sn catalyst in water, using this new cell type, will be reported, diffusional and mass transfer considerations which typically apply to gas/liquid/solid catalytic reactions will be addressed briefly.

2. Transport limitations

Carrying out catalytic reactions in the liquid phase – instead of the gas phase – results in some very important changes in physical characteristics which make diffusion and mass transfer very restrictive. Going from air to water viscosity increases by a factor of 50, making volumetric flow through a catalyst bed much more difficult. Diffusivity of oxygen decreases five orders of magnitude and a typical oxygen solubility is only 1 mol m^{-3} in water, a much lower concentration than 10 mol m^{-3} in normal air. Where the reactant to be oxidized generally is present in 1000 mol m^{-3} concentration, oxidation reactions carried out in water are generally rate limited by oxygen transfer and diffusion, especially the ones with economically sufficiently high rates. For a slurry reactor intra particle diffusion is generally more restrictive then oxygen transfer from the gas phase to the liquid phase or oxygen transfer from the liquid phase to the solid phase, i.e. the catalyst particle. For the EXAFS work, only intra particle diffusion in the wafer is considered, since only dissolved oxygen is used, and like in a slurry reactor, oxygen transfer from the liquid to the solid phase is generally less restrictive than intra particle diffusion.

An additional problem using spectroscopic characterization methods like EXAFS is caused by the increased volumetric density, going from air to water typically a factor of 1000, resulting in a higher absorbance of the matrix and restricting catalyst dilution which otherwise could be applied to overcome mass transfer and diffusional limitations.

In the following, three items will be discussed in more detail:

- (pre)treatment times needed to equilibrate or saturate catalyst particles and wafers;
- catalyst efficiency and sample homogeneity;
- minimal flow through a catalyst "bed" or wafer necessary to obtain uniform conditions during an oxidation reaction.

2.1. *Saturation time of catalyst samples*

Being interested in the effect of oxidative and reductive treatments on the catalyst structure, Van den Tillaart [3] calculated the time needed to saturate a certain catalyst body (Pt/graphite) by oxygen or by hydrogen considering gas diffusion from the saturated liquid into the wafer as the only transport mechanism. That is, the wafer surface is wetted by holding the wafer in a saturated liquid. Assuming instantaneous adsorption on the Pt-sites the following equation for the saturation time τ holds:

$$\tau = \frac{d_w^2 C_*}{8 D_e C_0} \quad \text{for} \quad \frac{C_0}{C_*} < 0.3. \tag{1}$$

Going from a reduced platinum site to an oxidized one

$$3O_2 + 4H_* \rightarrow 2H_2O + 4O_*, \quad (2)$$

a concentration of platinum surface atoms of 200 mol m^{-3} leads to C_*=150 mol m^{-3}. Using D_e= 5×10^{-10} m^2 s^{-1}, taking into account catalyst porosity and tortuosity, and C_0=1 mol m^{-3}, a saturation time of at least 10 h follows for a wafer of 10^{-3} m and 15 s for a 20 μm catalyst particle. When the catalyst is (pre)treated with hydrogen shorter times are found.

Obviously, working with wafers in the liquid phase is rather time consuming, while treatment in a free slurry enables quick handling.

2.2. *Catalyst efficiency and sample homogeneity*

Catalytic oxidations in liquid systems are generally carried out in three-phase reactors resulting in oxygen gradients from the gas to the bulk liquid, from the bulk liquid to the catalyst surface and inside the catalyst particle as shown in Fig. 1. Depending on the physical properties of the system, surface tension, hydrophobicity of the catalyst, etc., the catalyst particles can also be located at the gas–liquid interface making description more intricate. Only intra particle diffusion is considered here since, in most cases, it appears to be restrictive. For the estimation of the catalyst effectiveness factor η, and gradients inside the catalyst particle, the Weisz modulus, Φ, can be used (Froment and Bischoff [5]):

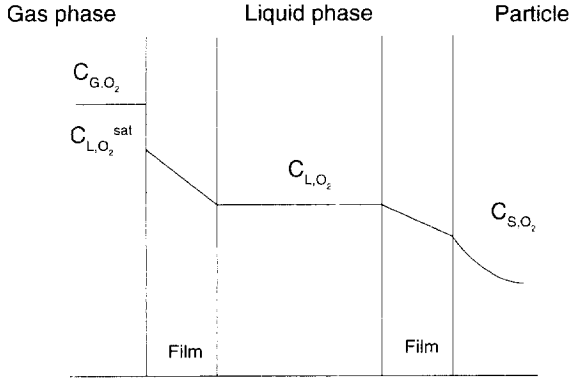

Fig. 1. Oxygen gradients in a stirred slurry reactor.

$$\Phi = \frac{n+1}{2}\left(\frac{V}{S}\right)^2 \frac{(r_v)_{obs}}{D_e C_0}. \quad (3)$$

The catalyst effectiveness factor, η, can be evaluated as a function of Φ. For sufficiently large Φ, the catalyst effectiveness factor η becomes inversely proportional to Φ:

$$\eta = \frac{1}{\Phi}. \quad (4)$$

The activity of most platinum catalysts used for the oxidation of alcohols in water lies within the range 10^{-3}–10^{-2} mol kg_{cat}^{-1} s^{-1} or within 1–10 mol $m_{cat.bed}^{-3}$ s^{-1}. The reaction order in oxygen generally varies from 0 to 1.

Substituting these values and the mentioned physical data in Eq. (3), results in

$$250 < \Phi < 5000 \text{ or } 2\times10^{-4} < \eta < 4\times10^{-3}$$

for 10^{-3} m wafers,

$$0.1 < \Phi < 2 \text{ or } 0.5 < \eta < 1 \quad \text{for } 20\,\mu\text{m particles.}$$

These values clearly show that using a wafer, the oxidation reaction only takes place in a very thin outside layer, resulting in an inhomogeneous catalyst sample, making EXAFS for the catalyst during oxidation useless. Wafers can only be applied at almost zero reaction rate or at equilibrium conditions. Using a packed bed of catalyst particles, a homogeneous sample can only be realized at low specific reaction rates and provided that sufficient dissolved oxygen can be transferred into the packed bed.

2.3. *Uniformity of O_2 concentration when flowing through a catalyst bed*

Passing oxygen saturated water through a catalyst bed where an oxidation reaction is taking place, the oxygen conversion usually will be high due to the low solubility of oxygen and due to the limited liquid velocity caused by a high flow resistance, i.e. the bed will not be operated in a differential way. If it is required that the gradient in oxygen concentration is less than 5%, i.e. $\Delta C_{O_2} < 0.05$ mol m^{-3}, over the catalyst bed of length L, being spotted with EXAFS, the minimal required superficial velocity, u_L, follows from

$$u_L \Delta C_{O_2} = L r_v. \quad (5)$$

Using a spot length of 10^{-3} m and a lower value for the reaction rate r_v of 1 mol m^{-3} s^{-1}, and assuming zero order in O_2 concentration, a minimal velocity of 2×10^{-2} m s^{-1} is obtained. Unfortunately with the catalysts used so far u_L was limited to approximately 1×10^{-2} m s^{-1}, due to a high pressure drop over the catalyst bed. For carrying out EXAFS characterization of a catalyst during reaction, a catalyst bed with a lower flow resistance is needed.

The considerations in Section 2 have pointed out that it is not possible yet to obtain reliable results from in situ EXAFS measurements, i.e. an EXAFS measurement while performing a reaction. However, it is possible to obtain reliable information by EXAFS of catalysts in the liquid phase after a (pre)treatment or a reaction. However, well-defined conditions for the catalyst are best met while measuring at an equilibrium state, i.e. conditions do not change during the EXAFS measurement. The EXAFS results, presented here, are limited to the investigation of the effect of (pre)treatments on the structure of Pt/Sn/C catalysts, measured at equilibrium conditions and using an EXAFS cell which was based on the considerations as discussed above.

3. Design of the EXAFS cell

Summarizing the transport considerations mentioned above it is clear that uniform catalyst conditions during catalyst treatments or reactions can be best met using a slurry reactor. A new EXAFS cell was developed allowing an on-line characterization procedure using a slurry reactor and hence, avoiding drying or contact to ambient conditions prior to EXAFS measurements. A schematic representation of this EXAFS cell is shown in Fig. 2. The cell, which is constructed mainly out of stainless steel, consists of a small compartment, sealed by mylar windows, which holds a millipore filter at the bottom side. After catalyst treatments in the slurry reactor, the catalyst slurry is pumped to the cell leaving a "bed" of catalyst, with a uniform density and composition, on the filter. The liquid is circulated back to the slurry reactor.

Cell construction parameters were based on the EXAFS spot size of $1\times10^{-3}\times1\times10^{-2}$ m and the specific cell width to obtain a total absorption of 2.5 for the sample. This leads to a width of 3×10^{-3} m for the cell used at the Pt L_{III}-edge and 3×10^{-2} m for the cell used at the Sn K-edge. The total cell volume was kept as small as possible to minimize the amount of catalyst needed. The catalyst slurry was brought back into the slurry reactor by holding the cell upside down followed by pumping water through the cell.

4. Experimental

4.1. Catalyst

The fresh platinum on high surface area graphite catalyst (Pt/C) was prepared according to the proce-

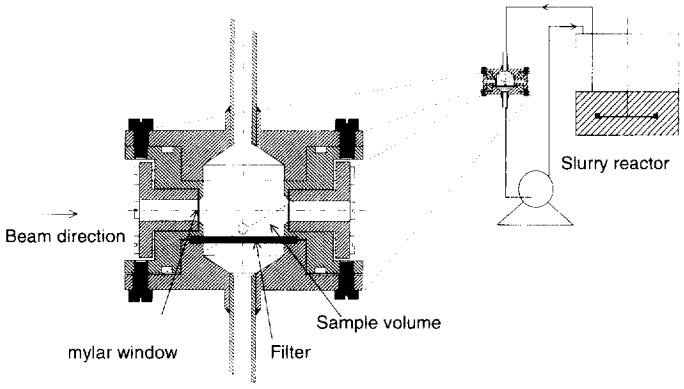

Fig. 2. Schematic representation of EXAFS cell and experimental setup used for on-line characterization.

dure of Richard and Gallezot [6]. Depending upon the batch the platinum content amounted to 3.8–4.4 wt% and the BET surface to 1.10×10^5 m^2 kg$_{cat}^{-1}$. The fraction of surface atoms Pt_s (%) as determined by CO chemisorption for these catalysts typically is 50%. Tin promotion was performed by adding a known amount of $SnCl_2{\cdot}2H_2O$ (Merck p.a.) to a slurry of catalyst which was reduced with hydrogen in ultra pure Millipore water (18 mW cm) at room temperature. Subsequently the catalyst was washed with 2×10^{-3} m^3 ultra pure Millipore water (18 mW cm) under nitrogen atmosphere. Tin was added in the ratio Pt_s:Sn=1 (mol/mol). Cyclic voltammetry showed that tin deposition was not only restricted to the platinum but also appeared on the graphite support [4]. Metal analysis showed that about 75% of the tin was deposited on the support.

4.2. Catalyst treatments

The treatments used for XAS characterization are described below. Table 1 lists the codes of the various samples after the treatments performed.

4.2.1. Non-dried samples

The non-dried aqueous samples HL and OL were all exposed, after preparation in the slurry reactor, to hydrogen saturated water in the slurry reactor for 15 min at ambient temperature.

- HL: Samples brought into the EXAFS cell still being exposed to hydrogen saturated water at ambient temperature.
- OL: Samples HL brought back into the slurry reactor after obtaining an EXAFS spectrum of the original and exposed to oxygen saturated water for 30 min. Hereafter the samples were brought in the EXAFS cell still being exposed to oxygen saturated water at ambient temperature.

Table 1
Overview of catalysts and treatments performed prior to EXAFS measurements

Catalyst	Treatments after preparation		Sample
Pt/C		HG	PtHG
Pt/Sn/C	Dried	AIR	PtSnDA
	Dried	HL	PtSnDHL
	Dried	OL	PtSnDOL
	Dried	HGT	PtSnDHGT
		HL	PtSnHL
		OL	PtSnOL

4.2.2. Dried samples

All samples referred to as D were filtered off after preparation and dried overnight at ambient conditions.

Gaseous treatments

- DA: Samples exposed to ambient conditions.
- DHG: Samples treated in situ with flowing hydrogen at atmospheric pressure and ambient temperature.
- DHGT: Samples treated with hydrogen gas at 573 K for 3 h and hereafter cooled down to 77 K still exposed to hydrogen.

Aqueous treatments. The aqueous samples, DHL and DOL, were all exposed ex situ to hydrogen saturated water at atmospheric pressure and 363 K. If the slurry reactor was used, the treatment was executed for 30 min. When exceptionally pressed wafers were used the treatment time was 24 h for the reasons given in Section 2.1.

1. DHL: Samples subsequently contacted in situ with hydrogen saturated water at atmospheric pressure and ambient temperature.
2. DOL: Samples ex situ exposed to oxygen saturated water at atmospheric pressure and ambient temperature and measured as such.

4.3. EXAFS data collection

EXAFS measurements were performed at station 9.2 of the SRS at Daresbury (UK) with an electron beam energy of 2 GeV and a stored current varying between 300 and 150 mA. The wiggler was operational at 5.0 T. Data were collected in the transmission mode at the Pt L_{III}-edge from 11.73 to 13.63 keV with a Si(2 2 0) monochromator detuned to 50% harmonic rejection.

Sn K-edge data were collected from 29.0 to 30.3 keV with a Si(2 2 0) monochromator. The ion chambers were filled with gas mixtures optimized to suit the measuring conditions. Energy calibration was monitored using either a platinum or tin foil and a third ion chamber and was set at 11.564 keV for the Pt L_{III}-edge and at 29.2 keV for the Sn K-edge.

4.4. XANES data analysis

The white line surface area was determined using the averaged XAS data of a sample. The Pt L_{III} and Pt L_{II}-edge regions were isolated, the energy rescaled to the edge, the pre-edge background was subtracted by using a Victoreen approximation and the data were finally normalized by the edge jump. The data were deconvoluted to the sum of an arctangent and a Lorentzian function as described by Horsley [7]:

$$\mu = \frac{1}{2} + \frac{1}{\pi}\arctan(p_1(E - p_2)) + \frac{p_3}{1 + p_4(E - p_5)^2}. \quad (6)$$

Maximum likelihood parameter estimates were obtained by applying a Marquardt algorithm to minimize the sum of squared residuals between the calculated and observed normalized absorption coefficient. The white line surface area was obtained as the integrated Lorentzian part of the regression function:

$$A = \int_{-\infty}^{\infty} \frac{p_3}{1 + p_4(E - p_5)^2}\,\mathrm{d}E = \frac{p_3\pi}{\sqrt{p_4}}. \quad (7)$$

The L_{II} surface area was corrected to the same scale as the L_{III} surface area by multiplication with the quotient of the specific edge jumps.

The white line surface area for the Pt L_{III}-edge has been used as a measure for the oxidation state. However, the white line surface area is sensitive to several factors: e.g. the presence of hydrogen, the oxidation state of the catalyst, the catalyst particle size, the support and the presence of a promoter metal. Lytle et al. [8,9] have e.g. shown for iridium, platinum and gold that the intensity of the white line of the L_{III} X-ray absorption edge is proportional to the d-electron vacancies. It is however important to examine both L_{III} and L_{II} edge before any statement about a change in electron density can be made.

Studying catalyst samples having the same support and having the same platinum particle size the relative changes in the white line surface area can be used as a diagnostic tool for the oxidation state of the catalyst, since as mentioned above the white line of the Pt L_{III} X-ray absorption edge is proportional to the d-electron vacancies.

4.5. EXAFS data analysis

Data analysis was performed using a computer program called XDAP which mainly follows the procedure described by Sayers and Bunker [10]. The pre-edge background was subtracted by using a Victoreen approximation. The EXAFS oscillations were isolated by background subtraction using a flexible spline approximation. Normalization was done by dividing the absorption intensities by the height of the absorption edge. The final chi-data were obtained by averaging the individual background subtracted and normalized EXAFS data. These chi-data were used to estimate adjustable parameters in the EXAFS model equation:

$$\hat{\chi}(k) = \sum_j \frac{N_j}{kR_j^2} F_j(k) \mathrm{e}^{-2k^2(\sigma^2)_j} \sin[2kR_j + \delta_j(k)]. \quad (8)$$

The photoelectron wave number, k, is defined for the jth shell as

$$k_j = \sqrt{\frac{8m\pi^2}{h^2}(E - E_0 - E_{c,j})}. \quad (9)$$

Phase shift and amplitude functions used here were extracted from reference compounds. Regression was performed by multiple shell fitting using a minimization routine incorporated into the program. The routine minimized the sum of square residuals between the observed and calculated EXAFS Fourier transforms of the chi-data, $\chi(k)$ and $\hat{\chi}(k)$.

5. Results and discussion

5.1. Structure of catalysts after treatment with aqueous hydrogen

5.1.1. Pt L_{III}-edge

Fig. 3 shows the k^2-weighed Fourier transforms of samples PtHG, PtSnHL and PtSnDHL. The sample PtHG is used since from earlier work performed by Van den Tillaart [2,3] it was already found that the structure of a Pt/C catalyst HL or HG is the same. The effects of tin promotion on the EXAFS signal are clear. Not only has the amplitude of the main peak of the Fourier transform changed, the relative amplitude of the different contributions has changed as well. Fig. 3

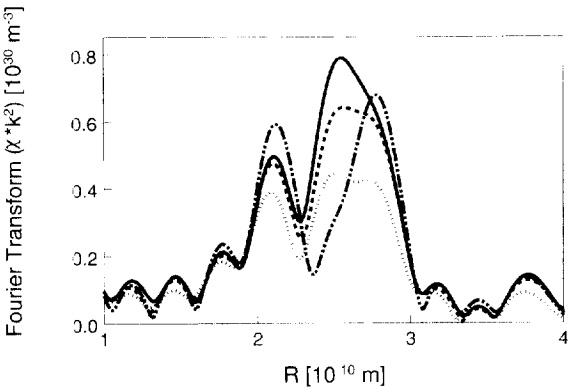

Fig. 3. Fourier transform of k^2-weighed raw Pt L_{III}-edge EXAFS data: PtHG (full line), PtSnHL (dotted line), PtSnDHL (dashed line) and PtSnDHGT (full/dashed line).

also shows a difference in the EXAFS signal obtained between an in situ treatment with aqueous hydrogen, PtSnHL, and a dried sample which hereafter has been treated with aqueous hydrogen, PtSnDHL. The change in the EXAFS signal is much stronger for sample PtSnHL. Parameter estimates of these samples are listed in Table 2. The sample PtHG can be described with a Pt–Pt contribution at 2.77×10^{-10} m and a Pt–C contribution at 2.62×10^{-10} m arising from the support. The samples PtSnHL and PtSnDHL both have a decreased Pt–Pt contribution at 2.75×10^{-10} m, an increased Pt–C contribution at 2.61×10^{-10} m and a Pt–Sn contribution at 2.65×10^{-10} m. The sample PtSnHL has a slightly higher Pt–Sn coordination number than PtSnDHL, but has a much lower Pt–Pt coordination number. A k^1 and k^3-weighed Fourier transform of the raw data and the data regressed, using Eq. (8), for sample PtSnHL is shown in Fig. 4. Regression was performed in r-space between 1.5×10^{-10} and 3×10^{-10} m. The deposition of tin on platinum is confirmed with both CO chemisorption as well as cyclic voltammetry [4]. The increased Pt–C coordination number for the tin promoted samples indicates possible spreading of the catalyst particle.

Using the white line surface area as a measure of the oxidation state of the catalyst, Van den Tillaart [2,3] already concluded from the white line area determined for sample PtHG compared with the same catalyst at ambient conditions that the platinum appeared to be reduced. The white line surface areas determined for the tin promoted catalysts are listed in Table 3. It is assumed that the particle size of the catalyst has not changed, although for sample PtSnHL the total Pt–metal coordination number is rather lower. Although no standard deviations are presented here, it appeared that the total platinum–metal coordination number was similar within experimental error for the samples. Therefore, comparing the white line surface area for samples under reducing and oxidizing conditions strongly indicates that the platinum of the tin promoted samples is also reduced under reducing conditions. Only small differences appear amongst the promoted samples.

These EXAFS results show, although the platinum appeared to be reduced equally, a remarkable difference in the EXAFS signal between the two tin promoted catalysts PtSnHL and PtSnDHL. The different

Table 2
Parameter estimates from the EXAFS analysis of Pt L_{III}-edge data for samples PtHG, PtSnHL, PtSnDHL and PtSnDHGT

Sample	Shell	N	$\Delta\sigma^2$ (10^{-25} m^2)	R (10^{-10} m)	$E_{c,i}$ (eV)
PtHG	Pt	7.94	377	2.765	5.28
	C	1.34	684	2.617	2.64
PtSnHL	Pt	4.79	352	2.750	6.77
	C	2.89	800[a]	2.612	9.62
	Sn	0.41	402	2.650	2.69
PtSnDHL	Pt	6.41	345	2.750	8.39
	C	3.11	800[a]	2.612	7.20
	Sn	0.30	340	2.650	8.78
PtSnDHGT	Pt	4.60	161	2.763	9.04
	C	3.82	800[a]	2.586	9.80
	Sn	2.67	519	2.730	1.38

[a]This parameter was kept constant during regression.

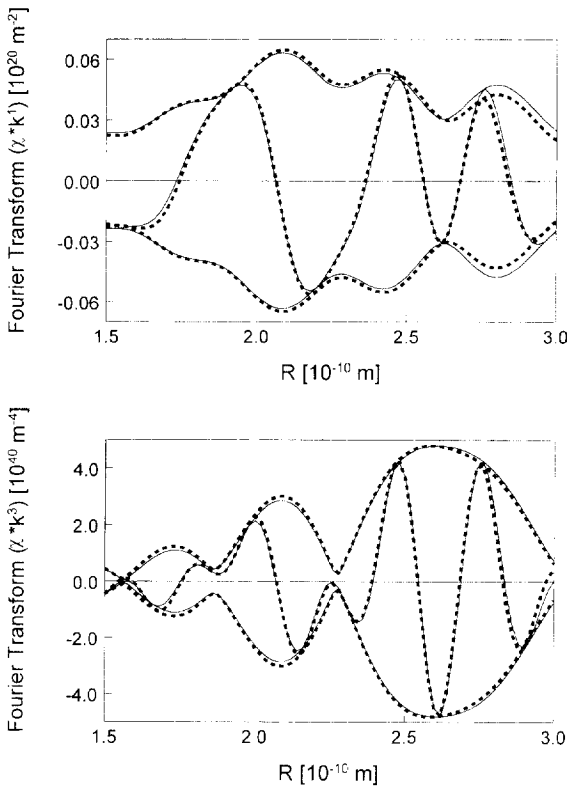

Fig. 4. EXAFS analysis Pt L_{III}-edge of sample PtSnHL. Full lines: observed data. Dashed lines: regressed using Eq. (8) – (a) k^1-weighed Fourier transform and (b) k^3-weighed Fourier transform.

Table 3
White line surface areas from deconvolution of the platinum L-edges for all samples

Sample	L_{III}-edge (eV)	L_{II}-edge (eV)
PtHG	7.66	0.48
PtSnHL	7.13	0.63
PtSnDHL	7.31	0.56
PtSnDHGT	7.72	0.65
PtSnOL	8.64	3.43
PtSnDOL	8.76	3.85

EXAFS signals could only be discovered since the new EXAFS cell enabled catalyst preparation and treatment avoiding contact to air.

5.1.2. Sn *K-edge*

Fig. 5 shows the k^1-weighed Fourier transform of samples PtSnHL and of PtSnDHL at the Sn K-edge.

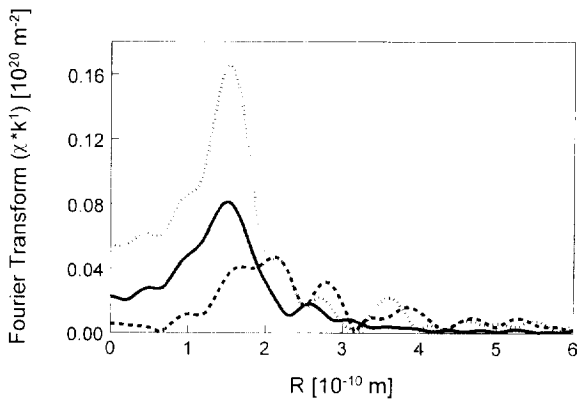

Fig. 5. Fourier transform of k^1-weighed raw Sn K-edge EXAFS data: PtSnHL (full line), PtSnDHL (dotted line) and PtSnDHGT (dashed line).

The differences between these two tin promoted samples are clear. The amplitude of the main peak at about 1.5×10^{-10} m is much lower for PtSnHL. The position of the peak between 2×10^{-10} and 3×10^{-10} m has shifted for sample PtSnHL to about 2.5×10^{-10} m. Parameter estimates, shown in Table 4, give a Sn–Pt contribution at 2.65×10^{-10} m for sample PtSnHL. The peak at 1.5×10^{-10} m derives from a Sn–O contribution at 2.05×10^{-10} m. The presence of a Sn–O contribution instead of a Sn–C contribution for sample PtSnHL indicates that the tin is bonded via oxygen to the graphite support. Parameter estimates for sample PtSnDHL only give a Sn–O contribution at 2.05×10^{-10} m with a much higher coordination number for oxygen than the Sn–O coordination number for PtSnHL. The occurrence of only a Sn–O coordination for sample PtSnDHL indicates that the major part of the tin deposited is still oxidized and could not be fully reduced. The absence of a Pt–O coordination at the Pt L_{III}-edge for sample PtSnDHL indicates that only the tin deposited on the platinum could be reduced. If it is kept in mind that the EXAFS signal originates from the total amount of tin deposited and the major part is deposited on the support, it can be understood why a Sn–Pt coordination could not be regressed significantly. Apparently the signal arising from tin present at the platinum surface showing Sn–Pt interactions is too small compared with the Sn–O signal from the tin present at the support. Once again these results show the necessity of the new EXAFS cell since, apparently,

Table 4
Parameter estimates from the EXAFS analysis of the Sn K-edge data for samples PtSnHL, PtSnDHL and PtSnDHGT

Sample	Shell	N	$\Delta\sigma^2$ (10^{-25} m^2)	R (10^{-10} m)	$E_{c,j}$ (eV)
PtSnHL	Pt	0.60	402	2.650	−3.89
	O	2.89	411	2.051	−1.36
PtSnDHL	O	4.86	96	2.065	−1.22
PtSnDHGT	Pt	2.51	326	2.709	−4.47
	O	1.02	330	2.088	5.11

exposure to ambient oxidizes the total amount of tin deposited to such an extent that the reductive treatments in aqueous phase used so far could not fully reduce tin. Due to the oxidized state of the tin deposited on the support, sample PtSnDHL reveals no Sn–Pt coordination.

5.2. *Structure of catalysts after treatment in aqueous oxygen*

5.2.1. Pt L_{III}-edge

Fig. 6 shows the k^2-weighed Fourier transforms of three samples: PtSnHL, PtSnOL and PtSnDOL. The samples PtSnOL and PtSnDOL have been treated with aqueous oxygen after a treatment with aqueous hydrogen. The effects of the oxidative treatment are clear from Fig. 6. The amplitude of the main peak at 2.5×10^{-10} m has decreased for sample PtSnOL and for PtSnDOL. These samples have an increase in the amplitude of the peak at about 1.6×10^{-10} m. The differences between the two tin samples are rather small.

Parameter estimates of sample PtSnOL and of PtSnDOL, Table 5, show a decreased Pt–Pt contribution at 2.75×10^{-10} m and the presence of a Pt–O contribution at 2.03×10^{-10} m. The parameter estimates point out that the two tin samples are oxidized to the same extent. The tin promoted catalysts are, however, more oxidized that a Pt/C catalyst is after an aqueous treatment [2,3], showing the sensitivity of tin for oxygen.

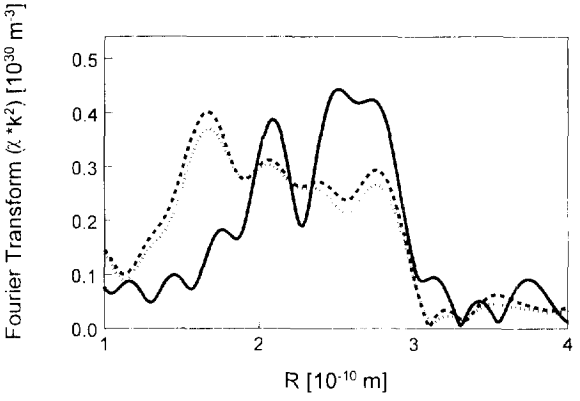

Fig. 6. Fourier transform of k^2-weighed raw Pt L_{III}-edge EXAFS data: PtSnHL (full line), PtSnOL (dotted line) and PtSnDOL (dashed).

This is confirmed with the white line surface area determination. Van den Tillaart [2,3] already stated the increase of the white line surface area for oxidized platinum catalysts. Table 3 clearly shows the increase in the white line surface area for both tin samples. It indicates the oxidized state of platinum in these catalysts and the negligible difference between the two tin samples PtSnOL and PtSnDOL.

Table 5
Parameter estimates from the EXAFS analysis of Pt L_{III}-edge data for samples PtSnOL and PtSnDOL

Sample	Shell	N	$\Delta\sigma^2$ (10^{-25} m^2)	R (10^{-10} m)	$E_{c,j}$ (eV)
PtSnOL	Pt	5.78	735	2.751	0.76
	O	1.88	515	2.037	10.46
PtSnDOL	Pt	5.48	651	2.758	0.42
	O	2.02	458	2.032	11.08

Table 6
Parameter estimates from the EXAFS analysis of Sn K-edge data for samples PtSnOL, PtSnDOL and PtSnDA

Sample	Shell	N	$\Delta\sigma^2$ (10^{-25} m^{-2})	R (10^{-10} m)	$E_{c,f}$ (eV)
PtSnOL	O	5.57	358	2.044	−0.63
PtSnDOL	O	5.77	81	2.064	−1.63
PtSnDA	O	5.64	106	2.061	−2.07

5.2.2. Sn *K-edge*

The EXAFS signals of PtSnOL and PtSnDOL appeared to be more or less similar. This appears also from the parameter estimates as shown in Table 6. Only a Sn–O coordination at 2.05×10^{-10} m could be found with comparable coordination numbers. Identical EXAFS results were obtained if these tin samples were exposed to ambient conditions (PtSnDA). The Sn–O coordination numbers found appear to be significantly higher than the Sn–O coordination number for sample PtSnDHL. This indicates that the aqueous reductive treatments result in reduction of only a small part of the total amount of deposited tin. Combining this observation with the results obtained for PtSnDHL at both Pt L_{III} and the Sn K-edge, it can be concluded that aqueous reductive treatments are capable of reducing tin deposited on platinum but not on the graphite support.

5.3. *Structure of catalysts after treatment with gaseous hydrogen at 573 K*

5.3.1. Pt L_{III}-*edge*

Fig. 3 shows, as mentioned earlier, the k^2-weighed Fourier transforms of sample PtHG, PtSnHL, PtSnDHL and of PtSnDHGT. The change in the EXAFS signal for PtSnDHGT is even more drastic compared to the other two tin samples PtSnHL and PtSnDHL. The main peak shape and position has clearly been changed. The relative amplitudes of the contributions have changed also. Parameter estimates of sample PtSnDHGT, shown in Table 2, give three contributions: Pt–Pt at 2.76×10^{-10} m, Pt–Sn at 2.73×10^{-10} m and Pt–C at 2.59×10^{-10} m. Both the extended Pt–Sn distance and the increased Pt–Sn coordination number indicate PtSn alloy formation. The white line surface area determination, as shown in Table 6, indicates once again that the platinum has been reduced.

5.3.2. Sn *K-edge*

Fig. 5 shows the k^1-weighed Fourier transform of sample PtSnHL, PtSnDHL and of PtSnDHGT at the Sn K-edge. The reductive treatment at 573 K has caused a large change in the EXAFS signal. The amplitude of the peaks has decreased drastically and the peaks have shifted in position. Parameter estimates give for PtSnDHGT a Sn–Pt coordination at 2.72×10^{-10} and a Sn–O at 2.05×10^{-10} m, shown in Table 4. These results confirm the tin bonding via oxygen to the support. The possible PtSn alloy formation is also confirmed since the Pt–Sn distance has increased as well as the Pt–Sn coordination number has.

6. Conclusions

A newly designed EXAFS cell enabling on-line characterization of catalysts used in the liquid phase, i.e. without drying, has been tested and used for studying tin promotion of a Pt/C catalyst. Moreover, a drastic reduction of (pre)treatment times was obtained using the developed cell. Tin promotion of a Pt/C catalyst leads to deposition of tin on both the platinum and the graphite support, tin being bonded via oxygen to the support. The tin promoted catalysts easily become oxidized in both gas and aqueous phase. A treatment with hydrogen at room temperature or in the liquid phase at 363 K only reduces the platinum and tin deposited on the platinum. Tin deposited on the graphite support however cannot be reduced. Therefore no significant Sn–Pt interaction could be concluded for dried catalyst treated with hydrogen at room temperature or in the aqueous phase at 363 K. Only after a severe reductive treatment at 573 K the initial structure was revealed again also indicating PtSn alloy formation. The effect of drying could only be revealed by using the newly developed EXAFS cell.

7. Notation

Roman symbols

A	normalized white line surface area, eV
C	concentration, mol m^{-3}
d	thickness, m
D	diffusion coefficient, $m^2 s^{-1}$
E	energy, eV
h	constant of Planck, J s
k	wave number, m^{-1}
L	bed length, m
m	electron mass, kg
N	number of atoms (dimensionless)
n	reaction order (dimensionless)
p	adjustable parameter (dimensionless)
R	coordination distance, m
r_v	volumetric reaction rate, mol $m^{-3} s^{-1}$
S	surface area of the particle, m^2
u	velocity, m s^{-1}
V	volume of the particle, m^3

Greek symbols

η	catalyst effectiveness factor (dimensionless)
$\hat{\mu}$	normalized absorption coefficient (dimensionless)
ν	stoichiometric number (dimensionless)
$\Delta\sigma^2$	relative mean square displacement, m^2
τ	saturation time, s
Φ	Weisz modulus (dimensionless)
$\hat{\chi}$	normalized modulation of absorption coefficient (dimensionless)

Functions

$\delta(k)$	phase shift function (dimensionless)
$\Phi(k)$	amplitude function, m

Subscripts

0	at boundary
c	correction
e	effective
j	of jth shell
L	superficial
obs	observations
w	wafer
*	adsorption sites

Acknowledgements

The EXAFS data were analyzed using a recently developed computer program XDAP (for information: XAFS services International, PO Box 24040, 3502 MA Utrecht, Netherlands). Thanks are due to the staff at the SRS (Daresbury) for technical support.

References

[1] T. Mallat, Z. Bodna, A. Baiker, J. Catal. 153 (1995) 131.
[2] J.A.A. Van den Tillaart et al., in: S.T. Oyama, J.W. Hightower (Eds.), Catalytic Selective Oxidation, ACS Symposium Series, vol. 523, American Chemical Society, Washington, DC, 1993, p. 298.
[3] J.A.A. Van den Tillaart, Platinum catalysis with oxygen in water. Catalyst characterization and kinetics of partial ethanol oxidation. Ph.D. Thesis, Eindhoven University of Technology, Eindhoven, 1994.
[4] F.A. Bruijn de, B.F.M. Kuster, G.B. Marin, Appl. Catal. A 145 (1996) 351.
[5] G.F. Froment, K.B. Bischoff, Chemical Reactor Analysis and Design, Wiley, New York, 1990.
[6] D. Richard, P. Gallezot, in: B. Delmon, P. Grange, P.A. Jacobs, G. Poncelet (Eds.), Preparation of Catalyst IV, Elsevier, Amsterdam, 1987, p. 71.
[7] J.A. Horsley, J. Chem. Phys. 76 (1982) 1451.
[8] F.W. Lytle, J. Catal. 43 (1976) 376.
[9] F.W. Lytle, P.S.P. Wei, B. Gregor, G.H. Via, J.H. Sinfelf, J. Chem. Phys. 70 (1979) 4849.
[10] D.E. Sayers, B.A. Bunker, in: D.C. Koningsberger, R. Prins (Eds.), X-ray Absorption: Principles, Applications, Techniques of EXAFS, SEXAFS and XANES, Wiley, New York, 1988, p. 211.